Equalization For Discrete Multitone Transceivers To Maximize Bit Rate

Güner Arslan, *Member, IEEE*, Brian L. Evans, *Senior Member, IEEE*, and Sayfe Kiaei, *Senior Member, IEEE*

Abstract

In a discrete multitone receiver, a time-domain equalizer (TEQ) reduces intersymbol interference (ISI) by shortening the effective duration of the channel impulse response. Current TEQ design methods such as minimum mean-squared error (MMSE), maximum shortening SNR (MSSNR), and maximum geometric SNR (MGSNR) do not directly maximize bit rate. In this paper, we develop two TEQ design methods to maximize bit rate. First, we partition an equalized multicarrier channel into its equivalent signal, noise, and ISI paths to develop a new subchannel SNR definition. Then, we derive a nonlinear function of TEQ taps that measures bit rate, which the proposed maximum bit rate (MBR) method optimizes. We also propose a minimum-ISI method that generalizes the MSSNR method by weighting the ISI in the frequency domain to obtain higher performance. The minimum-ISI method is amenable to real-time implementation on a fixed-point digital signal processor. Based on simulations using eight different carrier-serving-area loop channels, (1) the proposed methods yield higher bit rates than MMSE, MGSNR, and MSSNR methods; (2) the proposed methods give three-tap TEQs with higher bit rates than 17-tap MMSE, MGSNR, and MSSNR TEQs; (3) the proposed MBR method achieves the channel capacity (as computed by the matched filter bound) with a six-tap TEQ; and (4) the proposed minimum-ISI method achieves the bit rate of the optimal MBR method.

SP EDICS: *SP 3-TDSL: Telephone Networks and Digital Subscriber Loops*

G. Arslan performed this work at The Univ. of Texas at Austin, and is now with Cicada Semiconductor, Austin, TX 78704 USA, garslan@cicada-semi.com. B. L. Evans is with the Dept. of Electrical and Comp. Eng., The Univ. of Texas, Austin, TX 78712 USA, bevans@ece.utexas.edu. S. Kiaei performed this work at Motorola in Austin, and is now with the Dept. of Electrical Eng., Arizona State Univ., Tempe, AZ 85287 USA, Sayfe.Kiaei@asu.edu.

B. Evans was supported by a gift from Motorola. G. Arslan was sponsored by a Turkish Government Higher Education Council (YÖK) Fellowship administered by Yıldız Technical University, Istanbul, Turkey.

I. Introduction

Multicarrier modulation, particularly Discrete Multitone (DMT) modulation, is one of the most prominent modulation methods for high-speed digital communications. DMT partitions a broadband channel into a large number of virtually independent, narrowband subchannels. Ideally, each narrowband subchannel would have a flat frequency response and could be modeled as a gain plus additive white Gaussian noise (AWGN). The total number of bits transmitted over the broadband channel would be the sum of the bits transmitted in each narrowband subchannel.

Modulation by the Inverse Fast Fourier Transform (IFFT) and demodulation by the Fast Fourier Transform (FFT) create orthogonal subchannels. A spectrally shaped channel, however, destroys the orthogonality between subchannels so that they cannot be fully separated at the receiver, and causes both inter-carrier interference (ICI) and inter-symbol interference (ISI) [1]. One solution to prevent ISI is to add an appropriately long guard period at the beginning of each DMT symbol. When the guard period is a cyclic prefix, i.e. a copy of the last ν samples of a DMT symbol, ICI can be reduced.

Prepending a guard period of ν samples to each DMT symbol eliminates ISI when $\nu \geq L - 1$ [2], where L is the length of the channel impulse response. The guard period reduces the channel throughput by a factor of $N/(N + \nu)$, where N is both the symbol length and FFT length. When ν becomes large relative to N, this factor decreases so that the performance loss can be prohibitive. Hence, ν is chosen to be relatively small compared to N.

A channel shortening equalizer, commonly known as time-domain equalizer (TEQ), is required to shorten the length of the effective channel to the cyclic prefix length ν. The TEQ is a finite impulse response (FIR) filter. The equalized channel, which is the cascade of the channel and the TEQ, can be modeled as a delay by Δ samples followed by an FIR filter whose impulse response is the target impulse response (TIR) of $\nu + 1$ samples. The TIR would fit into a *target window* of $\nu + 1$ samples starting at sample index $\Delta + 1$ in the shortened impulse response (SIR). The rest of the SIR would ideally be zero.

Three major approaches for TEQ design require training sequences. The first approach minimizes the mean-squared error (MSE), where the error is the difference between the received symbol and desired symbol [3], [4], [5], [6], [7], [8]. The second approach estimates the channel impulse response and designs a TEQ that minimizes the energy of the impulse response outside of a target window, or equivalently, maximizes the shortening signal-to-noise ratio (SSNR) [9],

[10]. Neither the minimum MSE (MMSE) method nor the maximum SSNR (MSSNR) method directly maximizes the bit rate [11]. The third approach attempts to maximize bit rate by either optimizing an approximation to the geometric SNR (GSNR) [11], [12], [13], [14], or by optimizing the bit rate obtained by an adaptation algorithm [15].

The MMSE method [3] for TEQ design is based on a channel shortening method to decrease the complexity of Viterbi decoders [16] and is shown in Fig. 1. In Fig. 1, both the TEQ impulse response $\mathbf{w} = [w_0 \; w_1 \; \cdots \; w_{N_w-1}]^T$ and the target impulse response (TIR) $\mathbf{b} = [b_0 \; b_1 \; \cdots \; b_\nu]^T$ are finite in duration. If the error in Fig. 1 could be forced to be zero, then the SIR (upper path) would be equal to the TIR (lower path) with a time delay difference. By controlling the TIR length, we control the SIR length. Given the length of the TIR as $\nu + 1$, the goal is to find the TIR $\mathbf{b}$, delay Δ, and TEQ $\mathbf{w}$ that minimize the MSE. The lower path in Fig. 1 is not physically implemented but serves as a mechanism to calculate the TEQ.

The MMSE method prevents a trivial solution during optimization by placing a unit-tap constraint on the TIR $\mathbf{b}$ [3], [5], or a unit-energy constraint on either the TIR $\mathbf{b}$ or the TEQ impulse response $\mathbf{w}$. The unit-energy constraint gives a smaller MSE than a unit-tap constraint [6]. The optimal MMSE solution under the unit-energy constraint is the eigenvector corresponding to the minimum eigenvalue of a channel and noise dependent matrix [6], [16].

For the MMSE TEQ design method with a unit-energy constraint, iterative algorithms have been proposed to lower the computational cost, especially for the eigenvalue decomposition. Several algorithms discussed in [4] use frequency domain adaptation and time domain windowing to minimize the MSE. Although computationally efficient, these adaptive methods show slow convergence. Two fast iterative algorithms compute the minimum eigenvalue by using a modified power method [7] and Rayleigh minimization by exploiting asymptotic equivalence of Toeplitz and circulant matrices to estimate the Hessian matrix of a quadratic form [8].

The aforementioned MMSE methods do not have control over the frequency response of the TEQ. For example, a TEQ designed with these methods would have some gain over unused subchannels which would contribute only to the noise and not to the desired signal. Also, many MMSE optimal TEQs have deep nulls in the frequency domain. Those subchannels with deep nulls become useless. One solution to this problem is to add frequency weighted energy of the TEQ to the objective function (i.e. MSE) [17]. By placing a large positive weighting on unused subchannels, the energy in these subchannels can be minimized along with the MSE.

Another way to incorporate frequency domain control into the MMSE design method is per tone equalization [18]. Instead of having a TEQ followed later by a one-tap frequency domain equalizer (FEQ) for each subchannel, the TEQ is eliminated by a FEQ with multi-tap FIR filters. That is, the TEQ is mapped into the FEQ. This approach minimizes the MSE in each subchannel separately instead of minimizing the MSE in the time domain. Although this approach offers some frequency domain control, it is still based on minimizing the MSE and does not directly maximize bit rate.

The MSSNR method [9] is based on the observation that ISI is caused by the part of the SIR that lies outside of the target window. The SSNR is defined as the ratio of the energy of the SIR inside the target window to the energy outside of the target window [9]. The error definition in the MMSE approach includes this part of SIR but also includes the difference between the TIR and SIR inside the target window [10]. Therefore, minimizing the MSE does not necessarily minimize the SIR outside of the target window.

The MSSNR method directly minimizes the part of the SIR that causes ISI. This is a more effective method to reduce ISI than methods based on the MSE. The MSSNR method, however, uses only the channel impulse response when calculating the optimum TEQ, which means that it ignores the effect of the noise and transmit power spectrum. Since the bit rate is a function of noise, channel gain, and transmit power spectrum, a bit rate optimal TEQ design method must take into account all three when computing the optimum TEQ. As a consequence, the MSSNR method cannot optimize bit rate.

The Maximum GSNR (MGSNR) TEQ method [11] would maximize the bit rate if several restrictive conditions, ideal assumptions, and simplifications were to hold. Because the theoretical basis of the MGSNR TEQ method provides useful background information in the derivation of our proposed methods, we present the MGSNR method in Section II-B.

Instead of using a closed-form approximation for bit rate as in the MGSNR method, an alternate approach [15] uses an adaptation algorithm to calculate the bit rate for a given TEQ. This rather computationally complex adaptation algorithm returns the bit rate by using a mixture of time domain and frequency domain calculations. A multidimensional optimization method is used to optimize the bit rate. At every iteration of the optimization algorithm, the adaptation algorithm has to be used to calculate the bit rate.

We propose a new model for subchannel SNR that is based on the equivalent signal, noise, and

ISI paths of an equalized multicarrier channel [19]. We define the impulse response of the signal path as the part of the SIR lying inside the target window and the impulse response of the ISI path as the part of the SIR lying outside of the target window. We calculate the equivalent paths in the frequency domain by using the FFT and use this model to derive the optimal maximum bit rate (MBR) TEQ. The design of the optimal TEQ requires constrained nonlinear optimization which is impractical for cost-effective real-time implementations. Therefore, we propose a fast, near-optimal, minimum-ISI (min-ISI) method. The min-ISI method places the ISI in subchannels with high noise power.

The min-ISI method is intended for use in standard-compliant ADSL transceivers. These ADSL transceivers employ a periodic pseudo-noise training sequence followed later by an aperiodic pseudo-noise training sequence during initialization. The periodic training sequence consists of one fixed symbol without a cyclic prefix (the sequence is 1024 to 1536 symbols in the G.DMT standard). Although it is common for a receiver to use this sequence to train the TEQ, the standard does not require the TEQ to be designed at this point, nor does it prevent the TEQ from being modified or redesigned when receiving the aperiodic sequence. The aperiodic sequence is transmitted with a cyclic prefix. It is common for the receiver to use the aperiodic sequence to estimate the signal power and noise power in the subchannels of the equalized (shortened) channel. At the end of the aperiodic sequence, the receiver sends bit allocation information for each subchannel to the transmitter. In the G.DMT standard, the aperiodic sequence contains 16,384 symbols, and only a small portion of these symbols is necessary to determine the bit allocation. Hence, the first portion of symbols could be used to estimate the signal and noise power in each subchannel of the (unequalized) channel to generate the frequency weighting for the min-ISI method. Once the min-ISI method designs the TEQ, the TEQ could then be applied to the remaining aperiodic symbols to determine the bit allocation for the equalized channel.

We have implemented the min-ISI method (except for the frequency weighting) on three different fixed-point digital processors: Texas Instruments TMS320C6200 and TMS320C5000, and Motorola 56000. The source code is available at

http://www.ece.utexas.edu/~bevans/projects/adsl/index.html

The implementations are based on fast low-memory algorithms for the min-ISI and MSSNR methods [20]. Also on the above Web site, we have released a DMT TEQ design Matlab toolbox that implements the two proposed TEQ design methods and eight other TEQ design methods.

The toolbox is driven by a graphical user interface and may be extended to include other TEQ design methods.

The paper is organized as follows. Section II summarizes background information including the capacity of a multicarrier modulated channel, and the MGSNR TEQ design method. Section III presents the new model for subchannel SNR. Section IV derives the optimal MBR TEQ that maximizes the bit rate based on the new subchannel SNR model. Section V proposes the computationally efficient, near-optimal min-ISI method that generalizes the MSSNR method by weighting the ISI in the frequency domain. Section VI presents simulations results. In this section, we compare the performance of the proposed methods with the MMSE, MSSNR, and MGSNR methods and with channel capacity. Section VII concludes this paper.

II. Background

This section introduces necessary background information for the derivation of a new subchannel SNR definition in the next section and reviews the MGNSR TEQ design method. Section II-A defines the capacity and achievable bit rate of a multicarrier modulated channel. Section II-B describes the MGSNR TEQ method for maximizing an approximation to the achievable bit rate.

A. Capacity of a Multicarrier Channel

Modulation with a N-point IFFT generates two one-dimensional (real) (DC and Nyquist frequencies), and $N/2-1$ two-dimensional (complex) subchannels. For an adequately long cyclic prefix, it is reasonable to assume that the channel gain and noise power in each subchannel is flat. In this case, each subchannel can be modeled as an independent AWGN channel. The capacity of a multicarrier channel can be written in terms of bits per symbol as [2]

$$C_{DMT} = \sum_{i \in \mathcal{S}} \log_2 \left(1 + \mathrm{SNR}_i^{MFB}\right) \quad \text{bits/symbol} \tag{1}$$

The maximum achievable bits per symbol, on the other hand, can be written as

$$b_{DMT} = \sum_{i \in \mathcal{S}} \log_2 \left(1 + \frac{\mathrm{SNR}_i^{MFB}}{,}\right) \quad \text{bits/symbol} \tag{2}$$

where i is the subchannel index, $\mathcal{S}$ is the set of the indices of the used $\bar{N}$ subchannels out of $N/2+1$ subchannels, SNR_i^{MFB} is the matched filter bound of the SNR in the ith subchannel and is defined below in (3), and , is the SNR gap for achieving Shannon channel capacity and is assumed to be constant over all subchannels [21]. The bit rate can be calculated from (2) by

multiplying by the symbol rate, which is 4 kHz in the ADSL standards. In downstream G.DMT transmission, for example, the symbol rate is calculated as the sampling frequency (2.208 MHz) divided by samples per symbol (512+32=544) and multiplied by 68/69 to adjust for the fixed symbol in every frame of 69 symbols.

The SNR gap is a function of several factors, including the modulation method, allowable probability of error P_e, gain of any coding applied γ_{eff}, and desired system margin γ_m. The SNR gap can be approximated in the case of quadrature amplitude modulation (QAM) as [21]

$$, \approx \frac{\gamma_m}{3\gamma_{eff}} \left(Q^{-1} \left(\frac{P_e}{2} \right) \right)^2$$

Assuming that the input signal and noise are wide sense stationary, the SNR in the ith subchannel can be defined as

$$\mathrm{SNR}_i^{MFB} = \frac{S_{x,i}|H_i|^2}{S_{n,i}} \tag{3}$$

where $S_{x,i}$ and $S_{n,i}$ are the transmitted signal and channel noise power, respectively, and H_i is the gain of the channel spectrum in the ith subchannel. We also assume that the subchannels are narrow enough so that the channel frequency response and transmitted signal power spectrum are constant in each subchannel. The definition in (3) does not include the effect of ISI or any equalizer. It is the maximum achievable SNR or the matched filter bound (MFB). If the channel causes ISI or an equalizer has been used, then the definition has to be modified.

B. The Geometric TEQ Method

Al-Dhahir and Cioffi [11] propose a method to incorporate the optimization of achievable bit rate into the TEQ design. The goal is to use the ultimate performance measure as an objective function in the TEQ design procedure. Their derivation starts with the definition of the GSNR which is a useful measure related to the bit rate

$$\mathrm{GSNR} = , \left(\left[\prod_{i \in \mathcal{S}} \left(1 + \frac{\mathrm{SNR}_i^{EQ}}{,} \right) \right]^{1/\bar{N}} - 1 \right) \tag{4}$$

Maximizing the GSNR is equivalent to maximizing the bit rate [11]. In (4), the subchannel SNR defined in (3) is modified to include the effect of the equalizer [11]

$$\mathrm{SNR}_i^{EQ} = \frac{S_{x,i}|B_i|^2}{S_{n,i}|W_i|^2} \tag{5}$$

where $S_{x,i}$ is the signal power, $S_{n,i}$ is the noise power, and B_i and W_i are the gain of $\mathbf{b}$ and $\mathbf{w}$ in the ith subchannel, respectively.

Recall that the equalized channel can be modeled as a delay by Δ samples followed by an FIR filter whose impulse response is the TIR. Al-Dhahir and Cioffi state the optimum TIR problem as:

$$\mathbf{b}_{opt} = \arg\max_{\mathbf{b}} \sum_{i \in \mathcal{S}} \ln |B_i|^2 \text{ s.t. } \|\mathbf{b}\|^2 = 1 \text{ and } \mathbf{b}^T \mathbf{R}_{\boldsymbol{\Delta}} \mathbf{b} \leq \text{MSE}_{\max} \tag{6}$$

Here, $\mathbf{R}_{\boldsymbol{\Delta}}$ is a channel-dependent matrix and $\text{MSE}_{\max}$ is a channel-dependent parameter which limits the MSE. The nonlinear constrained optimization problem in (6) does not have a closed-form solution, but may be solved by numerical methods.

The MGSNR TEQ method is not optimum (in the sense of maximizing bit rate) due to several approximations. One approximation is in the GSNR definition itself— the method maximizes an approximation to the actual GSNR. The objective function is derived based on the assumption that the TIR and the TEQ coefficients are independent. However, this is not the case because the "optimal" TEQ coefficients are calculated from the "optimal" TIR coefficients using

$$\mathbf{w}_o^T = \mathbf{b}_o^T \mathbf{R}_{xy} \mathbf{R}_{yy}^{-1} \tag{7}$$

where $\mathbf{w}_o$ and $\mathbf{b}_o$ are the "optimal" TEQ and TIR vectors, respectively, and $\mathbf{R}_{xy}$ and $\mathbf{R}_{yy}$ the input-output cross-correlation and output autocorrelation, respectively.

The most important approximation, however, is in the definition of the subchannel SNR, SNR_i^{EQ} in (5), which includes the effect of the equalizer but not the effect of the ISI, even though the objective of the TEQ is to minimize ISI. This issue has been addressed [22] by modifying the SNR definition to include an ISI term:

$$\text{SNR}_i^{ISI} = \frac{S_{x,i}|B_i|^2}{S_{x,i}|B_i - W_i H_i|^2 + S_{n,i}|W_i|^2} \tag{8}$$

However, this modified definition is only used to evaluate the performance of the MGSNR TEQ method, which is still based on the definition given in (5).

In summary, the drawbacks of the MGSNR TEQ method are that

- its derivation is based on a subchannel SNR definition SNR_i^{EQ} that does not include the effect of ISI;
- it depends on the parameter MSE_{max} which has to be tuned for different channels;
- its objective function assumes that $\mathbf{b}$ and $\mathbf{w}$ are independent; and
- it requires a constrained nonlinear optimization solution.

Considerable effort has been spent to overcome the last issue listed above. Farhang-Boroujeny and Ding [14] propose an eigen-approach based sub-optimum solution to overcome the compu-

tational complexity of the constrained nonlinear optimization solver. This approach achieves similar performance with lower computational complexity. For some channels, this sub-optimum approach gives better performance, which proves that the MGSNR TEQ method is not optimum. Lashkarian and Kiaei [12] propose a projection onto convex sets method to iteratively solve the constrained nonlinear optimization problem with lower computational load. Chiu, Tsai, Liau and Troulis [13] reformulate the constrained nonlinear optimization method and propose an inverse power method to solve it. This approach also reduces computational complexity and in some cases gives better performance than the MGSNR TEQ method.

III. A Model for Subchannel SNR

In this section, we motivate the derivation of the equivalent impulse responses for the signal, ISI, and the noise path with an example, and use this derivation to model subchannel SNR.

A. Example: The Equivalent Impulse Responses for the Signal, ISI, and Noise Paths

Consider a DMT system with an FFT size of $N = 4$, and a cyclic prefix length of $\nu = 1$. Consider transmission of two DMT symbols $\mathbf{a} = [a_1\, a_2\, a_3\, a_4]$ and $\mathbf{b} = [b_1\, b_2\, b_3\, b_4]$ over an equalized channel $\tilde{h} = h * w$ as shown in Fig. 2. The length of the equalized channel $\tilde{h} = [\tilde{h}_1\, \tilde{h}_2\, \tilde{h}_3\, \tilde{h}_4]$ is four, and its delay is assumed to be $\Delta = 1$. Since the length of the equalized channel is longer than $\nu+1$, ISI will occur. With the addition of the cyclic prefix, the symbols become $\hat{\mathbf{a}} = [a_4\, a_1\, a_2\, a_3\, a_4]$ and $\hat{\mathbf{b}} = [b_4\, b_1\, b_2\, b_3\, b_4]$ which form the transmit sequence $\mathbf{x} = [\hat{\mathbf{a}}\, \hat{\mathbf{b}}]$.

The received signal $\mathbf{y} = \mathbf{x} * \tilde{\mathbf{h}} + \tilde{\mathbf{n}}$ can be expressed as:

$$
\begin{array}{r}
\text{delay} \rightarrow \\
\text{CP} \rightarrow \\
\\
\\
\\
\\
\\
\text{CP} \rightarrow \\
\\
\\
\\
\\
\text{tail} \rightarrow \\
\\
\end{array}
\begin{bmatrix} y_1 \\ y_2 \\ y_3 \\ y_4 \\ y_5 \\ y_6 \\ y_7 \\ y_8 \\ y_9 \\ y_{10} \\ y_{11} \\ y_{12} \\ y_{13} \end{bmatrix}
=
\begin{bmatrix}
\tilde{h}_1 a_4 & & & & & & & \\
\tilde{h}_1 a_1 & + & \tilde{h}_2 a_4 & & & & & \\
\tilde{h}_1 a_2 & + & \tilde{h}_2 a_1 & + & \tilde{h}_3 a_4 & & & \\
\tilde{h}_1 a_3 & + & \tilde{h}_2 a_2 & + & \tilde{h}_3 a_1 & + & \tilde{h}_4 a_4 & \\
\tilde{h}_1 a_4 & + & \tilde{h}_2 a_3 & + & \tilde{h}_3 a_2 & + & \tilde{h}_4 a_1 & \\
\tilde{h}_1 b_4 & + & \tilde{h}_2 a_4 & + & \tilde{h}_3 a_3 & + & \tilde{h}_4 a_2 & \\
\tilde{h}_1 b_1 & + & \tilde{h}_2 b_4 & + & \tilde{h}_3 a_4 & + & \tilde{h}_4 a_3 & \\
\tilde{h}_1 b_2 & + & \tilde{h}_2 b_1 & + & \tilde{h}_3 b_4 & + & \tilde{h}_4 a_4 & \\
\tilde{h}_1 b_3 & + & \tilde{h}_2 b_2 & + & \tilde{h}_3 b_1 & + & \tilde{h}_4 b_4 & \\
\tilde{h}_1 b_4 & + & \tilde{h}_2 b_3 & + & \tilde{h}_3 b_2 & + & \tilde{h}_4 b_1 & \\
 & & \tilde{h}_2 b_4 & + & \tilde{h}_3 b_3 & + & \tilde{h}_4 b_2 & \\
 & & & & \tilde{h}_3 b_4 & + & \tilde{h}_4 b_3 & \\
 & & \text{desired part} & & & & \tilde{h}_4 b_4 &
\end{bmatrix}
+
\begin{bmatrix} \tilde{n}_1 \\ \tilde{n}_2 \\ \tilde{n}_3 \\ \tilde{n}_4 \\ \tilde{n}_5 \\ \tilde{n}_6 \\ \tilde{n}_7 \\ \tilde{n}_8 \\ \tilde{n}_9 \\ \tilde{n}_{10} \\ \tilde{n}_{11} \\ \tilde{n}_{12} \\ \tilde{n}_{13} \end{bmatrix}
\tag{9}
$$

where $\tilde{\mathbf{n}}$ is the additive channel noise at the output of the equalizer, and '$*$' represents linear convolution. The received signal can be partitioned as follows:

- y_1: The equalized channel has a delay of one, the first received sample is invalid.
- y_2: The first transmitted sample is a cyclic prefix and is ignored.
- $y_3 - y_6$: These samples correspond to the first received DMT symbol $\tilde{\mathbf{a}}$.
- y_7: This sample is the cyclic prefix of the second symbol and is dropped.
- $y_8 - y_{11}$: These samples correspond to the second received DMT symbol $\tilde{\mathbf{b}}$.
- $y_{12} - y_{13}$: We have received all symbols transmitted, the remaining samples are invalid. They are caused by the duration of the channel impulse response.

In order to demodulate the received DMT symbols $\tilde{\mathbf{a}}$ and $\tilde{\mathbf{b}}$ correctly, the channel length has to be at most $\nu + 1 = 2$. Since the channel impulse response length in this example is four, the received symbols have an ISI component in addition to the desired signal component and the noise component

$$\mathbf{y} = \mathbf{x} * \tilde{\mathbf{h}}^{signal} + \mathbf{x} * \tilde{\mathbf{h}}^{ISI} + \tilde{\mathbf{n}} \tag{10}$$

where $\tilde{\mathbf{h}}^{signal}$ is the equivalent signal path impulse response and $\tilde{\mathbf{h}}^{ISI}$ is the equivalent ISI path impulse response.

- *The Desired Signal Component*: A cyclic prefix length of $\nu = 1$ sample prevents ISI for channels up to length $\nu + 1 = 2$. In the ideal case in which the channel is shortened to this length, the received symbols are the four-point circular convolution of the transmitted symbols and the channel impulse response. Then, the transmitted subsymbols can be recovered by dividing the received subsymbols by the channel frequency response (i.e. a one-tap FEQ). Therefore, the desired component of the received signal is

$$\mathbf{x} * \tilde{\mathbf{h}}^{signal} = \mathbf{x} * [0\,\tilde{h}_2\,\tilde{h}_3\,0] = [x_{delay}^{signal}\,a_{CP}^{signal}\,\mathbf{a}^{signal}\,b_{CP}^{signal}\,\mathbf{b}^{signal}\,x_{tail,1}^{signal}\,x_{tail,2}^{signal}] \quad (11)$$

where '*' represents linear convolution, x_{delay}^{signal} is the sample to be omitted due to the channel delay, a_{CP}^{signal} and b_{CP}^{signal} are the cyclic prefixes of the symbols $\mathbf{a}$ and $\mathbf{b}$, respectively, and $x_{tail,1}^{signal}$ and $x_{tail,2}^{signal}$ are the samples to be omitted due to the tail. Then, the received symbols are

$$\mathbf{a}^{signal} = \mathbf{a} \otimes \tilde{\mathbf{h}}^{signal} \quad (12)$$

$$\mathbf{b}^{signal} = \mathbf{b} \otimes \tilde{\mathbf{h}}^{signal} \quad (13)$$

where $\otimes$ represents circular convolution. All these terms are shown in (9).

- *The ISI Component*: All additional components outside the oval box in (9) are ISI terms and are due to the extra nonzero taps in the channel impulse response. The ISI terms can be written as follows:

$$\mathbf{x} * \tilde{\mathbf{h}}^{ISI} = \mathbf{x} * [\tilde{h}_2\,0\,0\,\tilde{h}_4] = [x_{delay}^{ISI}\,a_{CP}^{ISI}\,\mathbf{a}^{ISI}\,b_{CP}^{ISI}\,\mathbf{b}^{ISI}\,x_{tail,1}^{ISI}\,x_{tail,2}^{ISI}] \quad (14)$$

- *The Output Noise Component*: The last component of the received symbols corresponds to the additive noise $\tilde{\mathbf{n}}$ which is the filtered version of the channel noise by the equalizer. Therefore, the equivalent path for the noise consists only of the equalizer. That is,

$$\tilde{\mathbf{n}} = \mathbf{w} * \mathbf{n} = \mathbf{h}^{noise} * \mathbf{n}$$

The equivalent signal path impulse response $\mathbf{h}^{signal}$ and the equivalent ISI path impulse response $\mathbf{h}^{ISI}$ can be obtained from the equalized impulse response by using a window function $\mathbf{g}$ as

$$\mathbf{h}^{signal} = \tilde{\mathbf{h}} \odot \mathbf{g} = [\tilde{h}_1\,\tilde{h}_2\,\tilde{h}_3\,\tilde{h}_4] \odot [0\,1\,1\,0] = [0\,\tilde{h}_2\,\tilde{h}_3\,0]$$

$$\mathbf{h}^{ISI} = \tilde{\mathbf{h}} \odot (\mathbf{1} - \mathbf{g}) = [\tilde{h}_1\,\tilde{h}_2\,\tilde{h}_3\,\tilde{h}_4] \odot [1\,0\,0\,1] = [\tilde{h}_1\,0\,0\,\tilde{h}_4]$$

where $\odot$ represents element by element multiplication, and $\mathbf{g}$ is a zero vector everywhere except it is one for the $\nu + 1 = 2$ elements starting at index $\Delta + 1 = 2$ and $\mathbf{1}$ is a vector of all ones.

B. Generalization of the Equivalent Path Impulse Responses

The example in Section III-A can be generalized so that any received signal can be partitioned into the desired signal, ISI, and noise components. The signal and ISI components are linear filtered versions of the same transmitted signal. The filters can be obtained by partitioning the equalized channel impulse response. One of the filters is formed from the samples of the equalized channel inside the target window. We call this the equivalent signal path impulse response h_k^{signal}. The second filter is formed from the remaining samples of the equalized channel impulse response and is named the equivalent ISI path impulse response h_k^{ISI}.

In general, the two equivalent paths can be represented as:

$$\begin{aligned} h_k^{signal} &= \tilde{h}_k g_k \\ h_k^{ISI} &= \tilde{h}_k (1 - g_k) \end{aligned} \tag{15}$$

Here, $\tilde{h}_k = h_k * w_k$, h_k and w_k are the channel impulse response and TEQ, respectively, and

$$g_k = \begin{cases} 1 & \Delta + 1 \leq k \leq \Delta + \nu + 1 \\ 0 & \text{otherwise} \end{cases}$$

represents the target window.

Fig. 3(a)–(c) show a simulated channel, equalizer, and equalized channel (in continuous form for illustration purposes). Fig. 3(d)–(f) show the signal path, ISI path and the sum of both paths which is equal to the equalized channel. The equalizer could not shorten the channel to fit inside the target window. Therefore, a small part of the equalized channel acts as the equivalent ISI path impulse response.

The portion of the received signal corresponding to the additive noise of the channel is filtered by the equalizer. The equivalent noise impulse response is equal to the equalizer taps:

$$h_k^{noise} = w_k$$

Fig. 4 shows the original channel, the equalizer, and the three equivalent paths in an equalized channel.

C. New Definition of Subchannel SNR

As described in the previous section, the received signal consists of three components: the desired signal component, the ISI component, and the output noise component. The SNR can

be defined as:

$$\text{SNR} = \frac{\text{signal power}}{\text{noise power} + \text{ISI power}}$$

With this definition, we assume that ISI is a second additive noise source in the channel, which reduces the SNR in the same manner as channel noise does. This is an approximation that ignores the correlation between ISI and signal.

Using the equivalent path definitions, we define a new subchannel SNR, SNR_i^{NEW}, to incorporate both types of distortion as

$$\text{SNR}_i^{NEW} = \frac{S_{x,i}|H_i^{signal}|^2}{S_{n,i}|H_i^{noise}|^2 + S_{x,i}|H_i^{ISI}|^2} \tag{16}$$

where $S_{x,i}$, $S_{n,i}$, H_i^{signal}, H_i^{noise}, and H_i^{ISI} are the transmitted signal power, channel noise power (before the equalizer), signal path gain, noise path gain, and the ISI path gain in the ith subchannel, respectively. The equivalent path gains in subchannel i are the ith FFT coefficients of the equivalent path impulse responses.

When the channel is perfectly equalized to the desired length, the ISI path impulse response is equal to zero. In this case,

$$\begin{aligned} h_k^{signal} = \tilde{h}_k = h_k * w_k \quad &\rightarrow \quad H_i^{signal} = W_i H_i \\ h_k^{noise} = w_k \quad &\rightarrow \quad H_i^{noise} = W_i \\ h_k^{ISI} = 0 \quad &\rightarrow \quad H_i^{ISI} = 0 \end{aligned}$$

and the subchannel SNR ($SNR_i^{No\ ISI}$) can be written as

$$\text{SNR}_i^{No\ ISI} = \frac{S_{x,i}|W_i|^2|H_i|^2}{S_{n,i}|W_i|^2} = \frac{S_{x,i}|H_i|^2}{S_{n,i}} \tag{17}$$

This is equal to the MFB, SNR_i^{MFB}, given in (3) and is the maximum achievable SNR. This is expected since the SNR should be maximum when there is no ISI. Note that the second equality in (17) is valid only if $|W_i|$ is nonzero. For the subchannels in which $|W_i|$ is equal to zero, the equalizer stops the signal and noise which makes the definition of SNR meaningless.

To substitute H_i^{signal}, H_i^{ISI}, and H_i^{noise} in (16), N-point FFTs of h_k^{signal}, h_k^{ISI}, and h_k^{noise} are required. As a result of the convolution of the channel of length L and the equalizer of length N_w the length of h_k^{signal} and h_k^{ISI} is $L + N_w - 1$. Furthermore, the length of h_k^{noise} is equal to that of w_k, which is N_w.

To obtain length-N sequences, we either pad zeros (if the sequence is shorter than N) or drop the last few samples (if the sequence is longer than N). The TEQ is always shorter than N ($N_w < N$). The length of the SIR, however, may be longer than N. In practice, the channel impulse response would be calculated by taking the N-point IFFT of the channel frequency response which would result in a impulse response length of $L = N$. After convolving with the TEQ impulse response, the SIR would have a length of $N + N_w - 1$.

Under these assumptions, we need to pad zeros to the noise path impulse response (which is the TEQ impulse response). And we need to drop $N_w - 1$ samples from the signal and ISI path impulse responses. This process does not cause any error for the signal path impulse response since the target window is placed near the energy concentration of the SIR and the samples near the tail are already zeroed out. In the ISI path case, however, a small error is introduced by dropping the samples between indices $N + 1$ to $N + N_w - 1$. Our simulations show that the energy in the dropped samples is about 50 dB below the total energy of the ISI path impulse response. Since the SIR has most of its energy at the beginning of the response, this error is small and can be ignored.

IV. The Optimal Maximum-Bit-Rate (MBR) Equalizer

In this section, we develop a method for optimizing TEQ design for bit rate. To write the achievable bit rate in terms of the TEQ tap values, we derive the subchannel SNRs as a function of the TEQ taps. Including the zero padding and sample dropping mentioned in Section III-C, we rewrite the equivalent signal, ISI, and noise path impulse responses in matrix form as

$$\begin{aligned} \mathbf{h}^{signal} &= \mathbf{GHw} \\ \mathbf{h}^{ISI} &= \mathbf{DHw} \\ \mathbf{h}^{noise} &= \mathbf{Fw} \end{aligned} \tag{18}$$

where $\mathbf{h}^{signal}$, $\mathbf{h}^{ISI}$, and $\mathbf{h}^{noise}$ are length-N vectors representing the equivalent signal, ISI, and noise path impulse responses, respectively. The $N \times N_w$ matrix $\mathbf{H}$ is defined as the first N rows

of the convolution matrix of the channel,

$$\mathbf{H} = \begin{bmatrix} h_0 & 0 & 0 & \cdots & 0 \\ h_1 & h_0 & 0 & \cdots & 0 \\ \vdots & \vdots & \vdots & \ddots & \vdots \\ h_{N_w-1} & h_{N_w-2} & h_{N_w-3} & \cdots & h_0 \\ h_{N_w} & h_{N_w-1} & h_{N_w-2} & \cdots & h_1 \\ \vdots & \vdots & \vdots & \ddots & \vdots \\ h_{N-1} & h_{N-2} & h_{N-3} & \cdots & h_{N-N_w} \end{bmatrix}$$

$\mathbf{G}$ and $\mathbf{D}$ are $N \times N$ diagonal matrices representing the window function g_k and $1 - g_k$ defined as

$$\mathbf{G} = \mathrm{diag}(\overbrace{\underbrace{0, \cdots, 0}_{\Delta \text{ zeros}}, \underbrace{1, \cdots, 1}_{\nu+1 \text{ ones}}, 0, \cdots, 0}^{N \text{ elements}})$$

and

$$\mathbf{D} = \mathrm{diag}(\overbrace{\underbrace{1, \cdots, 1}_{\Delta \text{ ones}}, \underbrace{0, \cdots, 0}_{\nu+1 \text{ zeros}}, 1, \cdots, 1}^{N \text{ elements}})$$

where $\mathrm{diag}(\cdot)$ forms a diagonal matrix from its vector argument. The $N \times N_w$ matrix $\mathbf{F}$ is defined as

$$\mathbf{F} = \left[\begin{array}{c} \mathbf{I}_{N_w \times N_w} \\ \hline \mathbf{0}_{(N-N_w) \times N_w} \end{array} \right]$$

Here, $\mathbf{I}_{N_w \times N_w}$ represents an $N_w \times N_w$ unity matrix and $\mathbf{0}_{(N-N_w) \times N_w}$ represents an $(N - N_w) \times N_w$ matrix consisting of zeros. Define the FFT vector as

$$\mathbf{q}_i = \begin{bmatrix} 1 & e^{j2\pi i/N} & e^{j2\pi 2i/N} & \ldots & e^{j2\pi(N-1)i/N} \end{bmatrix}^T \tag{19}$$

so that the inner product of $\mathbf{q}_i^H$ with a N-point vector gives the ith FFT coefficient of that vector. Using (18) and (19),

$$\begin{aligned} H_i^{signal} &= \mathbf{q}_i^H \mathbf{G}\mathbf{H}\mathbf{w} \\ H_i^{ISI} &= \mathbf{q}_i^H \mathbf{D}\mathbf{H}\mathbf{w} \\ H_i^{noise} &= \mathbf{q}_i^H \mathbf{F}\mathbf{w} \end{aligned} \tag{20}$$

Finally, by substituting (20) in (16), we obtain

$$\mathrm{SNR}_i^{NEW} = \frac{S_{x,i} |\mathbf{q}_i^H \mathbf{G}\mathbf{H}\mathbf{w}|^2}{S_{n,i} |\mathbf{q}_i^H \mathbf{F}\mathbf{w}|^2 + S_{x,i} |\mathbf{q}_i^H \mathbf{D}\mathbf{H}\mathbf{w}|^2} \tag{21}$$

This definition includes the effects of both ISI and a TEQ.

Now our goal is to find the optimal TEQ which maximizes b_{DMT}. We rewrite (21) as

$$\mathrm{SNR}_i^{NEW} = \frac{\mathbf{w}^T\mathbf{H}^T\mathbf{G}^T\mathbf{q}_i S_{x,i}\mathbf{q}_i^H\mathbf{G}\mathbf{H}\mathbf{w}}{\mathbf{w}^T\mathbf{F}^T\mathbf{q}_i S_{n,i}\mathbf{q}_i^H\mathbf{F}\mathbf{w} + \mathbf{w}^T\mathbf{H}^T\mathbf{D}^T\mathbf{q}_i S_{x,i}\mathbf{q}_i^H\mathbf{D}\mathbf{H}\mathbf{w}} \tag{22}$$

$$= \frac{\mathbf{w}^T\mathbf{A}_i\mathbf{w}}{\mathbf{w}^T\mathbf{B}_i\mathbf{w}} \tag{23}$$

where

$$\begin{aligned}\mathbf{A}_i &= \mathbf{H}^T\mathbf{G}^T\mathbf{q}_i S_{x,i}\mathbf{q}_i^H\mathbf{G}\mathbf{H}\\ \mathbf{B}_i &= \mathbf{F}^T\mathbf{q}_i S_{n,i}\mathbf{q}_i^H\mathbf{F} + \mathbf{H}^T\mathbf{D}^T\mathbf{q}_i S_{x,i}\mathbf{q}_i^H\mathbf{D}\mathbf{H}\end{aligned}$$

Substituting this result into (2), we obtain

$$b_{DMT} = \sum_{i\in S}\log_2\left(1 + \frac{1}{,}\frac{\mathbf{w}^T\mathbf{A}_i\mathbf{w}}{\mathbf{w}^T\mathbf{B}_i\mathbf{w}}\right)\text{ bits/symbol} \tag{24}$$

which gives the achievable capacity as a function of the TEQ taps. Thus, we can maximize b_{DMT} using nonlinear optimization methods such as the quasi-Newton, conjugate gradient, or simplex algorithms [23]. The global optimum of this nonlinear optimization problem would give us the maximum bit rate (MBR) TEQ. In practice, however, we cannot guarantee convergence to the global optimum.

The only constraint required in (24) is $\mathbf{w} \neq \mathbf{0}$, which is to prevent the denominator from becoming zero. In practice, however, the constraint would be implemented by choosing a nonzero initial value for $\mathbf{w}$. Contrary to quadratic minimization problems in which the zero vector is the optimum solution, most optimization algorithms applied to (24) would not converge towards the zero vector because that would minimize bit rate by reducing the denominator term [23].

We do not consider the MBR TEQ method to be a practical solution to the equalization problem. Instead, we use it only as a benchmark for achievable performance. We use the Broyden-Fletcher-Goldfarb-Shanno quasi-Newton algorithm in Matlab's optimization toolbox (24) to find the MBR TEQ.

The model proposed in Section III leads to a nonlinear optimization problem to find the optimal MBR TEQ as in the MGSNR TEQ method [11] but with the following differences:

- The proposed subchannel SNR model includes the effect of ISI and no unrealistic assumptions are used to obtain the achievable capacity as a function of equalizer taps;

- No constraints are required for the new optimization problem, which enables the use of a variety of faster optimization methods;
- No ad-hoc parameters, such as MSE_{max}, need to be adjusted for different channels; and
- The MBR TEQ is directly obtained from the optimization, unlike the MGSNR TEQ method in which the equalizer is calculated using (7) after the TIR is obtained from the optimization.

V. The Near-Optimal Minimum-ISI (min-ISI) Equalizer

Calculating the MBR TEQ requires solving a nonlinear optimization problem. Even if a fast optimization algorithm were used, finding the global optimum can be a computationally expensive process. In order to use an equalizer in a practical system, we have to avoid nonlinear optimization. In this section, we propose the min-ISI equalizer which can be calculated without using a globally optimal constrained nonlinear optimization solver.

The idea behind the min-ISI method can be explained from (22). Both the numerator and the denominator of (22) are power terms. Since a power term is always nonnegative, minimizing the distortion power in each subchannel is equivalent to minimizing the sum of the distortion powers over all subchannels:

$$P_d(\mathbf{w}) = \sum_{i\in\mathcal{S}} \left(\mathbf{w}^T\mathbf{F}^T\mathbf{q}_i S_{n,i}\mathbf{q}_i^H\mathbf{F}\mathbf{w} + \mathbf{w}^T\mathbf{H}^T\mathbf{D}^T\mathbf{q}_i S_{x,i}\mathbf{q}_i^H\mathbf{D}\mathbf{H}\mathbf{w}\right)$$

After normalizing by $S_{n,i}$, we obtain

$$P_d^{norm}(\mathbf{w}) = \sum_{i\in\mathcal{S}} \mathbf{w}^T\mathbf{F}^T\mathbf{q}_i\mathbf{q}_i^H\mathbf{F}\mathbf{w} + \sum_{i\in\mathcal{S}} \mathbf{w}^T\mathbf{H}^T\mathbf{D}^T\mathbf{q}_i\left(\frac{S_{x,i}}{S_{n,i}}\right)\mathbf{q}_i^H\mathbf{D}\mathbf{H}\mathbf{w} \tag{25}$$

where $\mathbf{q}_i^H\mathbf{F}\mathbf{w}$ is the ith N-point FFT coefficient of $\mathbf{w}$. Thus, the first term in (25) is the square sum of the N-point FFT coefficients of $\mathbf{w}$, which is equal to the square sum of the coefficients of $\mathbf{w}$ due to Parseval's Theorem:

$$P_d^{norm}(\mathbf{w}) = \mathbf{w}^T\mathbf{w} + \mathbf{w}^T\mathbf{H}^T\mathbf{D}^T\sum_{i\in\mathcal{S}}\left(\mathbf{q}_i\frac{S_{x,i}}{S_{n,i}}\mathbf{q}_i^H\right)\mathbf{D}\mathbf{H}\mathbf{w} \tag{26}$$

The first term does not affect the minimization of (26) for a constant norm $\mathbf{w}$ (the optimal $\mathbf{w}$ can always be scaled to force $\mathbf{w}^T\mathbf{w} = 1$). While minimizing the distortion power, a constraint is required to prevent the minimization of the signal power as well. Therefore, we define the TEQ design problem as

$$\arg\min_{\mathbf{w}}\left(\mathbf{w}^T\mathbf{H}^T\mathbf{D}^T\sum_{i\in\mathcal{S}}\left(\mathbf{q}_i\frac{S_{x,i}}{S_{n,i}}\mathbf{q}_i^H\right)\mathbf{D}\mathbf{H}\mathbf{w}\right) \text{ s.t. } ||\mathbf{h}^{signal}||^2 = 1 \tag{27}$$

or alternatively as

$$\arg\min_{\mathbf{w}} \left(\mathbf{w}^T\mathbf{X}\mathbf{w}\right) \text{ s.t. } \mathbf{w}^T\mathbf{Y}\mathbf{w} = 1 \tag{28}$$

where

$$\begin{aligned}\mathbf{X} &= \mathbf{H}^T\mathbf{D}^T\sum_{i\in\mathcal{S}}\left(\mathbf{q}_i\frac{S_{x,i}}{S_{n,i}}\mathbf{q}_i^H\right)\mathbf{D}\mathbf{H}\\ \mathbf{Y} &= \mathbf{H}^T\mathbf{G}^T\mathbf{G}\mathbf{H}\end{aligned}$$

The constraint also ensures that the norm of the signal path impulse response is one. Hence, the output signal power is equal to the input signal power.

The proposed method in (27) is a generalization of the MSSNR method [9]. The constraints in both methods are equivalent in setting the norm of signal path impulse response to one. The MSSNR method minimizes the norm of the ISI path impulse response. The proposed method, on the other hand, minimizes a weighted sum of the ISI power, hence the name min-ISI. The weighting is with the inverse of the noise power. Both methods would be equivalent if the signal power to noise power ratio were constant for all subchannels and all subchannels (including the DC, Nyquist, and POTS splitter subchannels) were used.

In (27), the weighting by $S_{x,i}/S_{n,i}$ amplifies the objective function (which measures the ISI) in the subchannels with low noise power (high SNR). A small amount of ISI power in subchannels with low noise power can reduce the SNR in that subchannel dramatically, which in turn would reduce the bit rate. In subchannels with low SNR, however, the noise power is large enough to dominate the ISI power, so the effect of the ISI power on the SNR is negligible. This explains why the MSSNR method is not optimal in the sense of maximum channel capacity— it treats ISI in low and high SNR subchannels equally.

VI. Simulations

We present simulation results to analyze and compare the performance of the proposed MBR and min-ISI methods with the MMSE, MGSNR, and MSSNR methods. We use the eight standard carrier-serving-area (CSA) loops in Fig. 5 as our test channels. The channel data is generated using Linemod software [24]. All channel impulse responses consist of 512 samples sampled at a rate of 2.208 MHz. We add a fifth-order Chebyshev highpass filter with cutoff frequency of 5.4 kHz and passband ripple of 0.5 dB to each CSA loop to take into account the effect of the

splitter at the transmitter. The DC channel (channel 0), channels 1-5, and the Nyquist channel are not used.

We model the channel noise as -140 dBm AWGN distributed over the entire bandwidth plus near-end-cross-talk (NEXT) noise. The NEXT noise consists of 8 ADSL disturbers as described in the ANSI T1.413-1995 standard [25]. The input signal power is 23 dBm distributed equally over all used subchannels and the FFT size is set to $N = 512$.

Delay optimization has been applied by running all methods for all possible delays in the range of 1 to 50 samples, except for the methods based on optimization (MGSNR and MBR). The optimum delay as well as the initial point for the MGSNR TEQ method has been obtained from the MMSE method. That means that the MGSNR TEQ optimization starts with the optimal MMSE solution and delay. After experimenting with the constraint parameter MSE_{max} for the best performance of the MGSNR method, we set it to be 2 dB above the MSE obtained from the MMSE method. The optimum delay and the initial point for the MBR TEQ has been obtained from the min-ISI TEQ method. In the case when $N_w \geq \nu$, the method in [26] instead of the original MSSNR method in [9] is used.

Bandwidth optimization is applied by shutting down (i.e., by not assigning any transmit power to) subchannels with initial SNR lower than the required SNR to transmit two bits with a given SNR gap of $9.8 + 6 - 4.2 = 11.6$ dB. This corresponds to system margin of 6 dB and a coding gain of 4.2 dB. We are not using any bit loading algorithm, so all bit rate results are calculated from the SNR distribution after the TEQ is placed into the system. We assume that the power allocation is constant over all used subchannels and that it is not changed after the TEQ is placed into the system.

A. Performance versus number of equalizer taps N_w and cyclic prefix length ν

We analyze the performance of the aforementioned TEQ methods with respect to the number of equalizer taps N_w and cyclic prefix length ν. We first set $\nu = 32$ as dictated by the ADSL standard for downstream transmission and vary the number of taps in the TEQ N_w. This analysis is intended to give us insight about how many TEQ taps we need to obtain highest performance for all methods. The results are shown in Fig. 6.

Fig. 6 shows bit rate vs. N_w. Even though it is for CSA loop #4, it is representative of the performance of the TEQ design methods for the other standard CSA loops. The MBR and min-ISI methods achieve bit rates within 96% of the upper bound with only three TEQ taps.

For more than three TEQ taps, the bit rate of the MBR and min-ISI methods stays above 96% of the upper bound. On the other hand, the bit rate for MSSNR, MMSE, and MGSNR peaks, then declines, and then oscillates as N_w increases. MSSNR is only competitive with the MBR and min-ISI methods for very short TEQs ($N_w < 6$). For $N_w = 32$, the bit rate for MSSNR, MMSE, and MGSNR drops to 70% of the upper bound or less. The MBR and min-ISI methods can give higher bit rates than the other three methods for any TEQ size. The MBR and min-ISI methods give virtually the same performance, with the MBR method having a slightly better bit rate. The difference, however, would not be worth the extra effort of a nonlinear optimization required by the MBR method.

From Fig. 6, it might be concluded that for the min-ISI and MBR methods, a cyclic prefix of 32 is not required. Since large cyclic prefix reduces the throughput of the channel, we would like to find the smallest length under which the upper bound on bit rate can be achieved. To do so, we set $N_w = 17$ and vary ν from 2 to 36. The results are shown in Fig. 7.

In Fig. 7, the MBR and min-ISI methods achieve the maximum bit rate for a cyclic prefix of 11 samples when a 17-tap TEQ is used. The MGSNR method outperforms the MSSNR method (except for cyclic prefix lengths of 3, 13, and 14) and the MMSE method. The MGSNR method is only competitive with the MBR and min-ISI methods for short cyclic prefix lengths ($\nu \leq 8$). As ν increases, the bit rates achieved by the MSSNR, MGSNR, and MMSE methods essentially decrease, then increase, and finally decrease. The slope in the performance of the upper bound is caused by the bit rate reduction by the factor $\frac{N}{N+\nu}$ which is due to the increase in the cyclic prefix length.

Fig. 6 suggests that a three-tap equalizer can effectively shorten a channel. The objective of Fig. 8 is to find the smallest possible cyclic prefix length given a three-tap equalizer. With a three-tap equalizer, the MBR, min-ISI, and MSSNR methods achieve the upper bound on bit rate for $\nu = 25$. Using the min-ISI method, a three-tap equalizer and a cyclic prefix length of 25 can outperform all previously reported methods with up to 32 TEQ taps and a cyclic prefix length smaller than 36. The MMSE and the MGSNR TEQ methods are not competitive with the other methods for small N_w.

B. Achievable bit rates for the CSA loops

The bit rate results for all methods on all eight channels are listed in Table I for $N_w = 17$ equalizer taps and $\nu = 32$ cyclic prefix length, and Table II for $N_w = 3$ and $\nu = 32$. All results

are obtained by averaging over 25 measures.

Table I suggests that given a 17-tap equalizer, the bit rate losses are 30–57% for MMSE, 18–39% for MSSNR, and 6–32% for MGSNR, 1–2% for min-ISI, and less than 1% for MBR methods. Table II suggests that a three-tap equalizer can perform within 4% bit rate loss provided that either the minimum-ISI method or the MBR method is used to design it. For a three-tap equalizer, the bit rate losses are 3–8% for MSSNR, 29–39% for MGSNR, and 40–54% for MMSE methods.

The poor performance of the MMSE method can be explained as follows. The MMSE method minimizes the difference between the TIR and SIR. It minimizes both the difference inside the target window and outside the target window. Since the TIR is zero outside the window, minimizing the difference outside means forcing the SIR to lie inside the target window. However, the difference between the SIR and TIR inside the target window does not cause any ISI. Furthermore, the TIR and SIR has larger magnitude inside the target window than outside which means that difference between them inside the window causes the major part of the error. This means that the MMSE method primarily tries to minimize the difference inside the window, which does not cause ISI, than outside the window, which causes ISI. A TEQ which has larger MSE caused by the difference inside the target window could give better performance than one that gives smaller MSE only caused by difference outside the target window. Therefore, minimizing the MSE is not a good choice to design a TEQ for discrete multitone modulation.

The MGSNR TEQ method is the first approach to include a channel capacity maximization into the TEQ design procedure. However, with all the approximations in formulating the GSNR, a constraint on the MSE is required to achieve good performance. This constraint forces the method to converge to a solution close to that of the MMSE method.

Since ISI is caused only by the part of the SIR outside the target window, minimizing only the part outside seems to be a good direction to take. The MSSNR method gives the optimal solution in the sense of minimizing the energy of the SIR outside the target window. This solves the problem with the MMSE method but is still not optimal as shown in the simulations. It is, in general, not possible to force the SIR to lie entirely inside a target window with an FIR TEQ. We show that the part outside the target window act as an equivalent ISI path. The frequency response of the ISI path determines which frequency bins are going to carry the ISI power by what amount. The distribution of this ISI power changes the SNR distribution, which changes

the achievable bit rate. The MSSNR method, however, does not consider the shape of the SIR lying outside the target window, but only the energy.

Although the derivation of our min-ISI method is based on maximizing the bit rate, it is a generalization of the MSSNR method. The proposed minimum-ISI method weights the residual ISI in frequency to penalize ISI in high SNR subchannels. With this weighting, the energy lying outside the target window is not necessarily minimum anymore, but the bit rate will be higher.

VII. Conclusion

We present a new subchannel SNR definition based on our derivation of equivalent signal, noise, and ISI paths in a DMT system. Based on the subchannel SNR definition, we derive the channel capacity as a nonlinear function of equalizer taps. We develop an optimal maximum bit rate (MBR) solution, which requires constrained nonlinear optimization and thus is not cost effective for a real-time system. The MBR method achieves close the upper bound on channel capacity as computed by the matched filter bound. To reduce computational complexity, we derive a near-optimal min-ISI method that is a generalization of the maximum shortening SNR (MSSNR) method with the addition of a frequency domain weighting of the ISI power.

In simulations, both the MBR and min-ISI methods outperform previously reported MMSE, MSSNR, and MGSNR methods in bit rate. The min-ISI method delivers virtually equal performance to that of the MBR method. A three-tap TEQ designed by either of the two proposed methods outperforms 17-tap equalizers designed by MMSE, MSSNR, and MGNSR TEQ methods.

Acknowledgements

The authors would like to thank Mr. Ming Ding (UT Austin), Mr. Milos Milosevic (Schlumberger and UT Austin), and the reviewers for their useful suggestions and comments on the paper. The authors would also like to thank the following seniors at UT Austin for implementing the Minimum ISI Method on programmable digital signal processors: Mr. David J. Love (djlove@ece.utexas.edu) on the TI TMS320C6000; Mr. Jerel Canales (jerelcan@yahoo.com) and Mr. Scott Margo (scomargo@yahoo.com) on the TI TMS320C5000; and Mr. Wade Berglund (wadeberglund@yahoo.com) on the Motorola 56000. The programmable digital signal processor implementations are based on fast low-memory algorithms for the Minimum ISI method developed for a senior design project at UT Austin by Mr. Jeff Wu (jeffwu78@stanford.edu) [20].

References

[1] J. A. C. Bingham, "Multicarrier modulation for data transmission: An idea whose time has come," *IEEE Comm. Magazine*, vol. 28, pp. 5–14, May 1990.

[2] T. Starr, J. M. Cioffi, and P. J. Silverman, *Understanding Digital Subscriber Line Technology.* Prentice-Hall PTR, 1999.

[3] J. S. Chow and J. M. Cioffi, "A cost-effective maximum likelihood receiver for multicarrier systems," in *Proc. IEEE Int. Conf. Comm.*, vol. 2, (Chicago, IL), pp. 948–952, June 1992.

[4] J. S. Chow, J. M. Cioffi, and J. A. Bingham, "Equalizer training algorithms for multicarrier modulation systems," in *Proc. IEEE Int. Conf. Comm.*, vol. 2, (Geneva, Switzerland), pp. 761–765, May 1993.

[5] I. Lee, J. S. Chow, and J. M. Cioffi, "Performance evaluation of a fast computation algorithm for the DMT in high-speed subscriber loop," *IEEE J. on Selected Areas in Comm.*, vol. 13, pp. 1564–1570, Dec. 1995.

[6] N. Al-Dhahir and J. M. Cioffi, "Efficiently computed reduced-parameter input-aided MMSE equalizers for ML detection: A unified approach," *IEEE Trans. on Info. Theory*, vol. 42, pp. 903–915, May 1996.

[7] M. Nafie and A. Gatherer, "Time-domain equalizer training for ADSL," in *Proc. IEEE Int. Conf. Comm.*, vol. 2, (Montreal, Canada), pp. 1085–1089, June 1997.

[8] N. Lashkarian and S. Kiaei, "Fast algorithm for finite-length MMSE equalizers with application to discrete multitone modulation," in *Proc. IEEE Int. Conf. Acoust., Speech, and Signal Processing*, vol. 5, (Phoenix, AR), pp. 2753–2756, Mar. 1999.

[9] P. J. W. Melsa, R. C. Younce, and C. E. Rohrs, "Impulse response shortening for discrete multitone transceivers," *IEEE Trans. on Comm.*, vol. 44, pp. 1662–1672, Dec. 1996.

[10] M. Webster and R. Roberts, "Adaptive channel truncation for FFT detection in DMT systems - error component partitioning," in *Proc. IEEE Asilomar Conf. on Signals, Systems, and Computers*, vol. 1, (Pacific Grove, CA), pp. 669–673, Nov. 1997.

[11] N. Al-Dhahir and J. M. Cioffi, "Optimum finite-length equalization for multicarrier transceivers," *IEEE Trans. on Comm.*, vol. 44, pp. 56–63, Jan. 1996.

[12] N. Lashkarian and S. Kiaei, "Optimum equalization of multicarrier systems via projection onto convex set," in *Proc. IEEE Int. Conf. Comm.*, vol. 2, (Vancouver, Canada), pp. 968–972, June 1999.

[13] W. Chiu, W. K. Tsai, T. C. Liau, and M. Troulis, "Time-domain channel equalizer design using the inverse power method," in *Proc. IEEE Int. Conf. Comm.*, vol. 2, (Vancouver, Canada), pp. 973–977, June 1999.

[14] B. Farhang-Bouroujeny and M. Ding, "Design methods for time-domain equalizers in DMT transceivers," *IEEE Trans. on Comm.*, vol. 49, pp. 554–562, Mar. 2001.

[15] W. Henkel and T. Kessler, "Maximizing the channel capacity of multicarrier transmission by suitable adaptation of the time-domain equalizer," *IEEE Trans. on Comm.*, vol. 48, pp. 2000–2004, Dec. 2000.

[16] D. D. Falconer and F. R. Magee, "Adaptive channel memory truncation for maximum likelihood sequence estimation," *Bell System Technical J.*, vol. 52, pp. 1541–1562, Nov. 1973.

[17] B. Wang, T. Adalı, Q. Liu, and M. Vlaynic, "Generalized channel impulse response shortening for discrete multitone transceivers," in *Proc. IEEE Asilomar Conf. on Signals, Systems, and Computers*, vol. 1, (Pacific Grove, CA), pp. 276–280, Nov. 1999.

[18] K. V. Acker, G. Leus, M. Moonen, O. V. D. Wiel, and T. Pollet, "Per tone equalization for DMT-based systems," *IEEE Trans. on Comm.*, vol. 49, pp. 109–119, Jan. 2001.

[19] G. Arslan, B. L. Evans, and S. Kiaei, "Optimum channel shortening for discrete multitone transceivers," in *Proc. IEEE Int. Conf. Acoust., Speech, and Signal Processing*, (Istanbul, Turkey), June 2000.

[20] J. Wu, G. Arslan, and B. L. Evans, "Efficient matrix multiplication methods to implement a near-optimum channel shortening method for discrete multitone transceivers," in *Proc. IEEE Asilomar Conf. on Signals, Systems, and Computers*, (Pacific Grove, CA), Nov. 2000.

[21] J. M. Cioffi, *A Multicarrier Primer.* Amati Communication Corporation and Stanford University, T1E1.4/91-157, Nov. 1991.

[22] N. Al-Dhahir and J. M. Cioffi, "Bandwidth-optimized reduced-complexity equalized multicarrier transceiver," *IEEE J. on Selected Areas in Comm.*, vol. 45, pp. 948–956, Aug. 1997.

[23] W. H. Press, S. A. Teukolsky, W. T. Vetterling, and B. P. Flannery, *Numerical Recipes in C.* New York, NY: Cambridge University Press, 2 ed., 1992.

[24] D. G. Messerschmitt, "LINEMOD - a transmission line modeling program," 1999. Web: http://www-isl.stanford.edu/people/cioffi/linemod/linemod.html.

[25] "Network and customer installation interfaces - assymmetric digital subscriber line (ADSL) metallic interface, T1.413-1995," 1995. American National Standards Institute, NY.

[26] C. Yin and G. Yue, "Optimal impulse response shortening for discrete multitone transceivers," *IEE Electronics Letters*, vol. 34, pp. 35–36, Jan. 1998.

Güner Arslan received his BSEE degree in July 1994 from Yıldız University (now known as Kocaeli University) in Kocaeli, Turkey, his MSEE degree in July 1996 from Yıldız Technical University in Istanbul, Turkey, and his Ph.D. degree in December 2000 from The University of Texas at Austin. His MS thesis was on stereophonic acoustic echo cancellation (advisor was Prof. F. Ayhan Sakarya). At Yıldız, he also worked on real-time DTMF detection, neural networks for beamforming, automated fingerprint analysis, and SAR image processing. In 1997, he received a Turkish Government Higher Education Council (YÖK) Fellowship administered by Yıldız Technical University for graduate study abroad and enrolled at UT Austin in the Spring of 1998. At UT Austin, his Ph.D. dissertation was on time-domain equalization for discrete multitone transceivers (advisor was Prof. Brian L. Evans). His research interests are in digital signal processing for communications, audio/speech applications, and learning systems (neural networks, genetic algorithms, and adaptive filters). He currently works as a Design Engineer at Cicada Semiconductor in Austin, TX, in physical layer transceiver design.

Brian L. Evans received his BSEECS degree from the Rose-Hulman Institute of Technology in May 1987, and his MSEE and Ph.D. degrees from the Georgia Institute of Technology in December 1988 and September 1993, respectively. From 1993 to 1996, he was a post-doctoral researcher at the University of California at Berkeley where he worked on electronic design automation for embedded systems as a member of the Ptolemy project. He is the primary architect of the *Signals and Systems Pack* for Mathematica, which has been on the market since October of 1995.

He is currently a tenured Associate Professor in the Department of Electrical and Computer Engineering at The University of Texas at Austin. He enjoys conducting research and teaching courses in embedded real-time signal and image processing systems. His current research focuses on the design and real-time implementation of ADSL/VDSL transceivers, desktop printer pipelines, video codecs, and 3-D sonar imaging systems. He has published more than 90 refereed journal and conference papers on these topics. He developed and currently teaches Multidimensional Digital Signal Processing, Embedded Software Systems, and Real-Time Digital Signal Processing Laboratory. Dr. Evans is an Associate Editor of the *IEEE Transactions on Image Processing*, a member of the Design and Implementation of Signal Processing Systems Technical Committee of the IEEE Signal Processing Society, and the recipient of a 1997 National Science Foundation CAREER Award.

Sayfe Kiaei received his Ph.D. in 1987 from Washington State University. He has been with Arizona State University since January 2001. He is currently Professor in the Department of Electrical Engineering and the Director of Communications & Mixed-Signals Research Center. He was with Motorola Inc. from 1993–2001 as a Senior Member of Technical Staff with the Wireless Technology Center, and Broadband Operations at Motorola responsible for the development of Wireless Transceiver IC's. Prior to that, he was with the Broadband

Products Operations responsible for research and development of xDSL systems design. Before joining Motorola, he was a faculty member at Oregon State University where he taught Digital Communications, VLSI system design, DSP, communications, advanced CMOS IC design, and wireless systems.

His research area is in telecommunications, VLSI and DSP development. Dr. Kiaei assisted in the establishment of the Industry-University Center for the Design of Analog/Digital IC's (CDADIC), and served as a Co-Director of CDADIC for 10 years. Prior to this, he was employed at Boeing's Flight Systems Research and Technology Center as Hardware Design Engineer and CAD tool development for airplane controllers. Dr. Kiaei has received four major research awards, and was presented the Carter Best Teacher Award by students and faculty of Oregon State College of Engineering. He is the recipient of IEEE's Darlington Award for the best paper in the *IEEE Transactions on Circuits and Systems* for a paper on low-noise circuits for mixed-signal IC's. Dr. Kiaei is a Senior Member of the IEEE and has served in various editorial capacities for the society. He has been active in numerous conference events as conference chairman, technical program chair, or member of technical program committees. He has published over 50 journal and conference papers and patents.

List of Tables

I Achievable bit rates for the eight CSA loops equalized with the MMSE [6], MGSNR [12], MSSNR [11], the proposed min-ISI, and the proposed MBR methods, in percentage with respect to the maximum achievable bit rate in the case of no ISI or equivalently with an SNR equal to the matched filter bound (MFB). $N_w = 17$, $\nu = 32$, $N = 512$, coding gain = 4.2 dB, margin = 6 dB, input power = 23 dBm, AWGN power -140 dBm/Hz, NEXT noise modeled as 8 ADSL disturbers. 29

II Achievable bit rates for the eight CSA loops equalized with the MMSE [6], MGSNR [12], MSSNR [11], the proposed min-ISI, and the proposed MBR methods, in percentage with respect to the maximum achievable bit rate in the case of no ISI or equivalently with an SNR equal to the matched filter bound (MFB). $N_w = 3$, $\nu = 32$, $N = 512$, coding gain = 4.2 dB, margin = 6 dB, input power = 23 dBm, AWGN power -140 dBm/Hz, NEXT noise modeled as 8 ADSL disturbers. 30

List of Figures

1 Block diagram of the minimum mean-squared error (MMSE) equalizer 29

2 Example: Two DMT symbols $\mathbf{a}$ and $\mathbf{b}$ are transmitted over an equalized channel $\tilde{\mathbf{h}} = \mathbf{h} * \mathbf{w}$. After dropping the invalid samples and the cyclic prefixes, the two symbols are received as $\tilde{\mathbf{a}}$ and $\tilde{\mathbf{b}}$. 30

3 The impulse responses of a channel (a), equalizer (b), and the equalized channel (c). Partition of the equalized channel impulse response into the signal path (d) and ISI path (e). The sum of signal and ISI paths (f) is equal to the equalized channel impulse response (c). 31

4 Block diagrams for the equalized channel and the corresponding signal, noise, and ISI paths in a DMT system. 32

5 Configuration of the eight standard CSA loops. Numbers represent length/thickness in feet/gauge. The vertical lines represent bridge taps. 33

6 Achievable bit rate versus the number of equalizer taps for CSA loop 4, $\nu = 32$, $N = 512$, coding gain = 4.2 dB, margin = 6 dB, input power = 23 dBm, AWGN power -140 dBm/Hz, NEXT noise modeled as 8 ADSL disturbers. As N_w increases, the bit rate should be monotonically increasing if the method is guaranteed to find the optimum bit rate. For the MSSNR, MMSE, and MGSNR methods, the dependence of bit rate on N_w is not monotonic. 34

7 Achievable bit rate versus the cyclic prefix length ν for CSA loop 4, $N_w = 17$, $N = 512$, coding gain = 4.2 dB, margin = 6 dB, input power = 23 dBm, AWGN power -140 dBm/Hz, NEXT noise modeled as 8 ADSL disturbers. 35

8 Achievable bit rate with respect to cyclic prefix length ν for CSA loop 4, $N_w = 3$, $N = 512$, coding gain = 4.2 dB, margin = 6 dB, input power = 23 dBm, AWGN power -140 dBm/Hz, NEXT noise modeled as 8 ADSL disturbers. 36

	achievable percentage of MFB bit rate					bit rate
loop	MMSE	MGSNR	MSSNR	min-ISI	MBR	MFB
1	43%	84%	62%	99%	99%	9.059 Mbps
2	70%	73%	75%	98%	99%	10.344 Mbps
3	64%	94%	82%	99%	99%	8.698 Mbps
4	70%	68%	61%	98%	99%	8.695 Mbps
5	61%	84%	72%	98%	99%	9.184 Mbps
6	62%	93%	80%	99%	99%	8.407 Mbps
7	57%	78%	74%	99%	99%	8.362 Mbps
8	66%	90%	71%	99%	100%	7.394 Mbps

TABLE I

ACHIEVABLE BIT RATES FOR THE EIGHT CSA LOOPS EQUALIZED WITH THE MMSE [6], MGSNR [12], MSSNR [11], THE PROPOSED MIN-ISI, AND THE PROPOSED MBR METHODS, IN PERCENTAGE WITH RESPECT TO THE MAXIMUM ACHIEVABLE BIT RATE IN THE CASE OF NO ISI OR EQUIVALENTLY WITH AN SNR EQUAL TO THE MATCHED FILTER BOUND (MFB). $N_w = 17$, $\nu = 32$, $N = 512$, CODING GAIN = 4.2 DB, MARGIN = 6 DB, INPUT POWER = 23 DBM, AWGN POWER −140 DBM/HZ, NEXT NOISE MODELED AS 8 ADSL DISTURBERS.

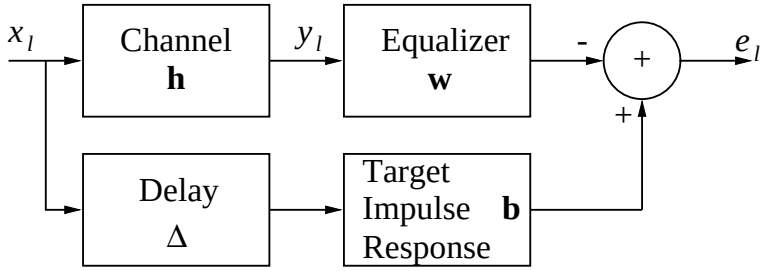

Fig. 1. Block diagram of the minimum mean-squared error (MMSE) equalizer

	achievable percentage of MFB bit rate					bit rate
loop	MMSE	MGSNR	MSSNR	min-ISI	MBR	MFB
1	54%	70%	96%	97%	98%	9.059 Mbps
2	47%	71%	96%	96%	97%	10.344 Mbps
3	57%	69%	92%	98%	99%	8.698 Mbps
4	46%	66%	97%	97%	98%	8.695 Mbps
5	52%	65%	96%	97%	98%	9.184 Mbps
6	60%	71%	95%	98%	99%	8.407 Mbps
7	46%	63%	93%	96%	97%	8.362 Mbps
8	55%	61%	94%	98%	99%	7.394 Mbps

TABLE II

ACHIEVABLE BIT RATES FOR THE EIGHT CSA LOOPS EQUALIZED WITH THE MMSE [6], MGSNR [12], MSSNR [11], THE PROPOSED MIN-ISI, AND THE PROPOSED MBR METHODS, IN PERCENTAGE WITH RESPECT TO THE MAXIMUM ACHIEVABLE BIT RATE IN THE CASE OF NO ISI OR EQUIVALENTLY WITH AN SNR EQUAL TO THE MATCHED FILTER BOUND (MFB). $N_w = 3$, $\nu = 32$, $N = 512$, CODING GAIN = 4.2 DB, MARGIN = 6 DB, INPUT POWER = 23 DBM, AWGN POWER −140 DBM/HZ, NEXT NOISE MODELED AS 8 ADSL DISTURBERS.

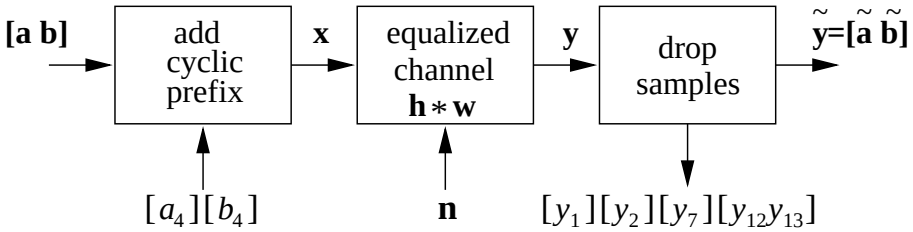

Fig. 2. Example: Two DMT symbols $\mathbf{a}$ and $\mathbf{b}$ are transmitted over an equalized channel $\tilde{\mathbf{h}} = \mathbf{h} * \mathbf{w}$. After dropping the invalid samples and the cyclic prefixes, the two symbols are received as $\tilde{\mathbf{a}}$ and $\tilde{\mathbf{b}}$.

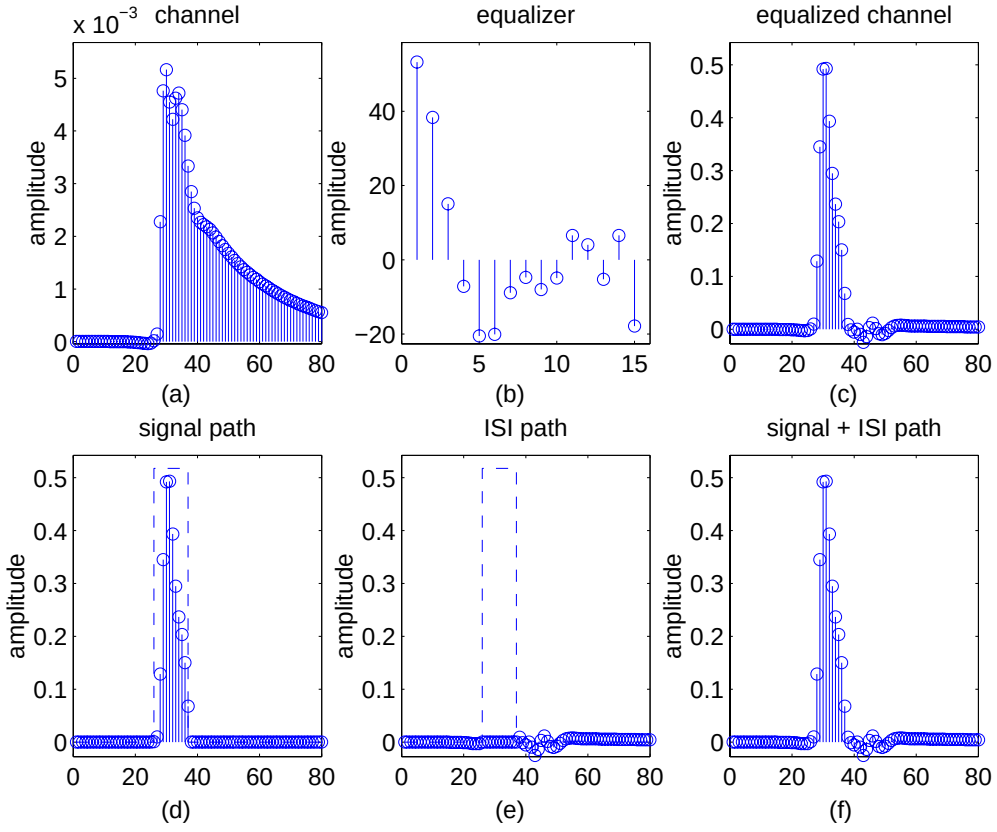

Fig. 3. The impulse responses of a channel (a), equalizer (b), and the equalized channel (c). Partition of the equalized channel impulse response into the signal path (d) and ISI path (e). The sum of signal and ISI paths (f) is equal to the equalized channel impulse response (c).

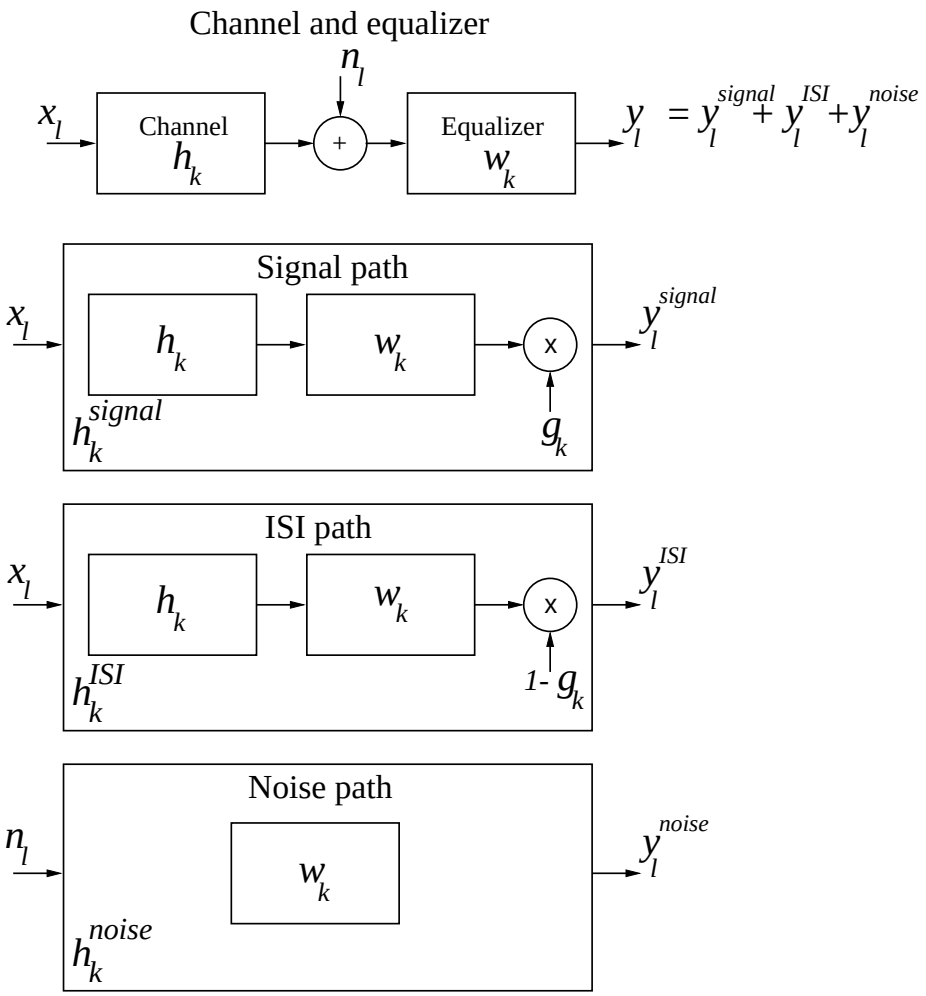

Fig. 4. Block diagrams for the equalized channel and the corresponding signal, noise, and ISI paths in a DMT system.

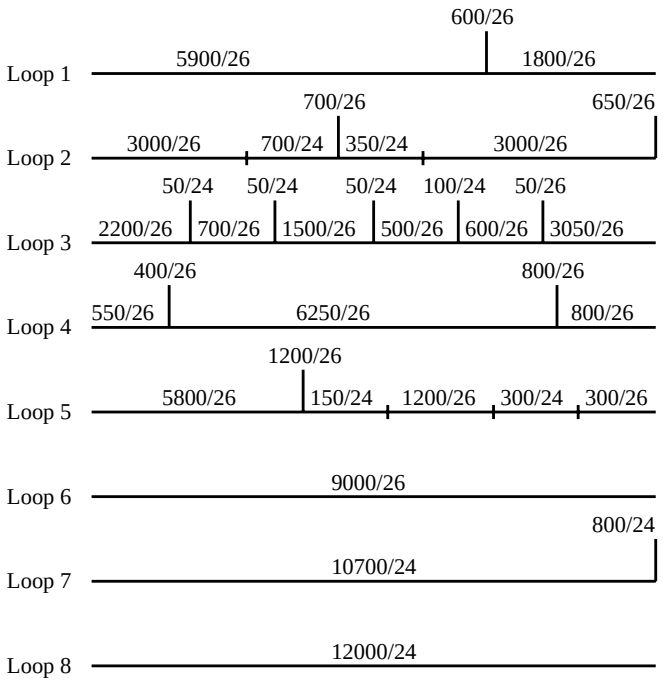

Fig. 5. Configuration of the eight standard CSA loops. Numbers represent length/thickness in feet/gauge. The vertical lines represent bridge taps.

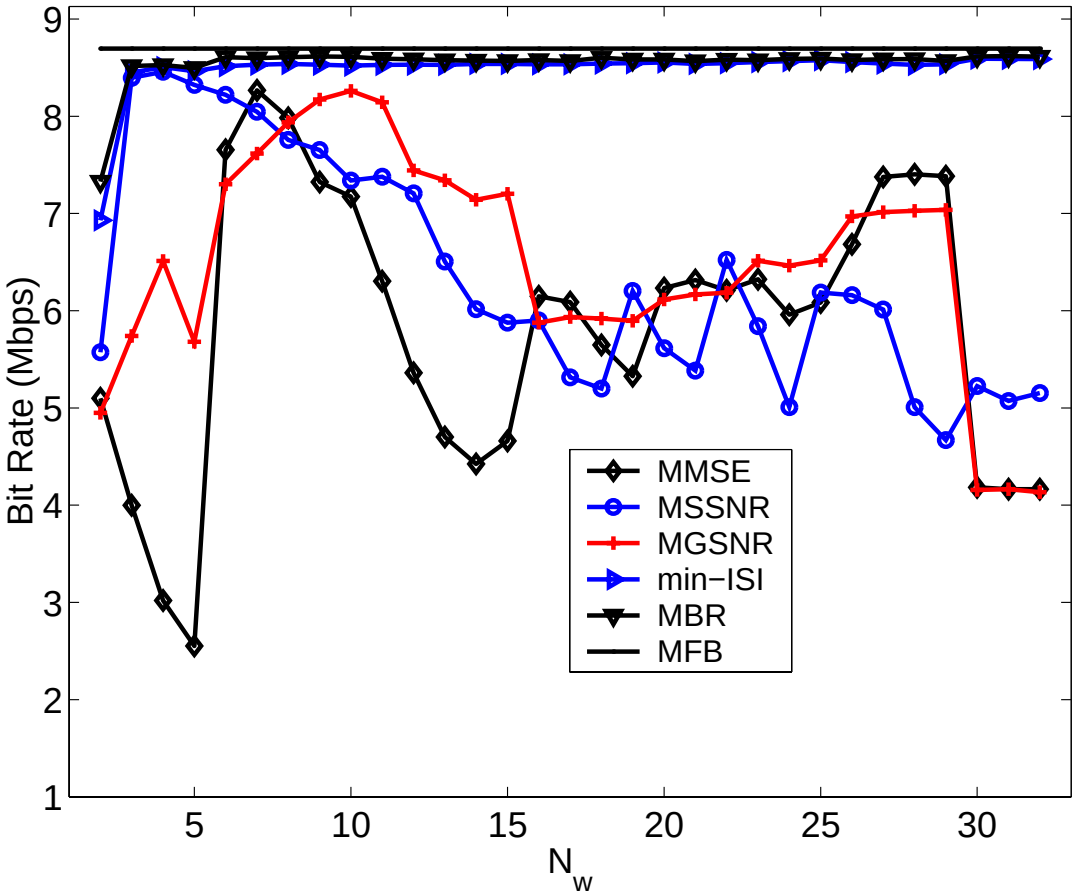

Fig. 6. Achievable bit rate versus the number of equalizer taps for CSA loop 4, $\nu = 32$, $N = 512$, coding gain = 4.2 dB, margin = 6 dB, input power = 23 dBm, AWGN power −140 dBm/Hz, NEXT noise modeled as 8 ADSL disturbers. As N_w increases, the bit rate should be monotonically increasing if the method is guaranteed to find the optimum bit rate. For the MSSNR, MMSE, and MGSNR methods, the dependence of bit rate on N_w is not monotonic.

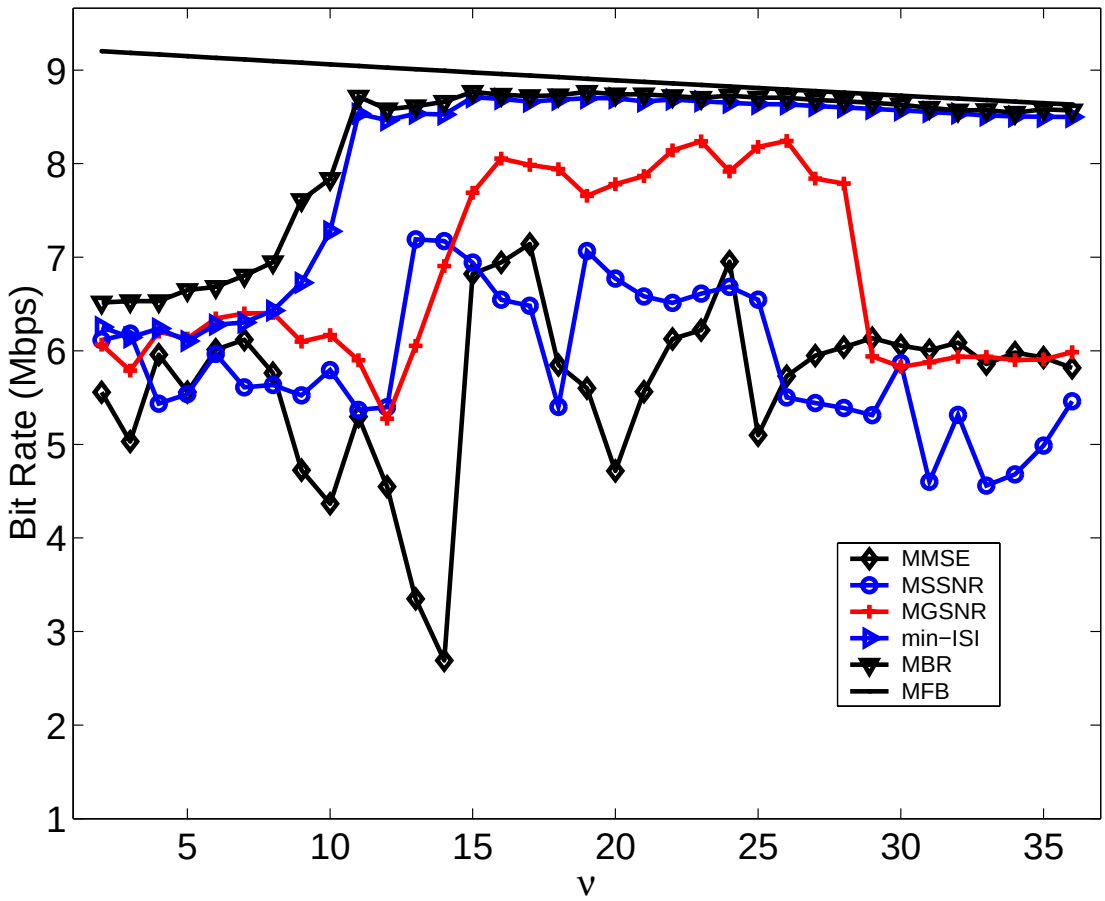

Fig. 7. Achievable bit rate versus the cyclic prefix length ν for CSA loop 4, $N_w = 17$, $N = 512$, coding gain = 4.2 dB, margin = 6 dB, input power = 23 dBm, AWGN power −140 dBm/Hz, NEXT noise modeled as 8 ADSL disturbers.

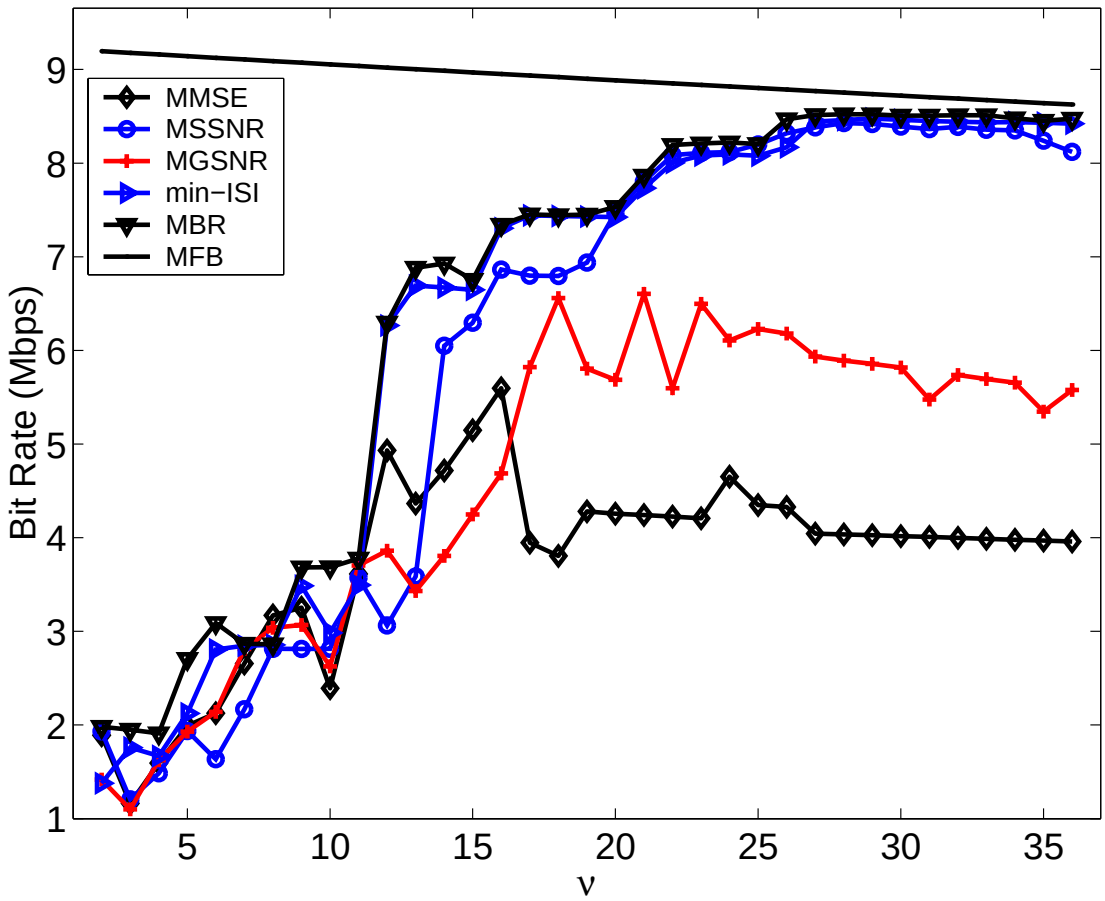

Fig. 8. Achievable bit rate with respect to cyclic prefix length ν for CSA loop 4, $N_w = 3$, $N = 512$, coding gain = 4.2 dB, margin = 6 dB, input power = 23 dBm, AWGN power −140 dBm/Hz, NEXT noise modeled as 8 ADSL disturbers.